HAL
open science

# How vial geometry variability influences heat transfer and product temperature during freeze-drying

Bernadette Scutella, Stéphanie Passot, Erwan Bourlés, Fernanda Fonseca, Ioan-Cristian Trelea

## To cite this version:

Bernadette Scutella, Stéphanie Passot, Erwan Bourlés, Fernanda Fonseca, Ioan-Cristian Trelea. How vial geometry variability influences heat transfer and product temperature during freeze-drying. Journal of Pharmaceutical Sciences, 2017, 106 (3), pp.770-778. 10.1016/j.xphs.2016.11.007 . hal-01465155

**HAL Id: hal-01465155**

**https://hal.science/hal-01465155v1**

Submitted on 10 Feb 2017

**HAL** is a multi-disciplinary open access archive for the deposit and dissemination of scientific research documents, whether they are published or not. The documents may come from teaching and research institutions in France or abroad, or from public or private research centers.

L'archive ouverte pluridisciplinaire **HAL**, est destinée au dépôt et à la diffusion de documents scientifiques de niveau recherche, publiés ou non, émanant des établissements d'enseignement et de recherche français ou étrangers, des laboratoires publics ou privés.

# How vial geometry variability influences heat transfer and product temperature during freeze-drying

Authors: BERNADETTE SCUTELLA[1,2], STEPHANIE PASSOT[1], ERWAN BOURLES[2], FERNANDA FONSECA[1], IOAN CRISTIAN TRELEA[1]

[1] UMR GMPA, AgroParisTech, INRA, Université Paris Saclay, 78850 Thiverval-Grignon, France

[2] GSK Vaccines, Rixensart, Belgium

**ABSTRACT:** Vial design features can play a significant role in heat transfer between the shelf and the product and, consequently, in the final quality of the freeze-dried product. Our objective was to investigate the impact of the variability of some geometrical dimensions of a set of tubing vials commonly used for vaccine production on the distribution of the vial heat transfer coefficients ($K_v$) and its potential consequence on product temperature. Sublimation tests were carried out using pure water and eight combinations of chamber pressure (4 to 50 Pa) and shelf temperature (-40 °C and 0 °C) in two freeze-dryers. $K_v$ values were individually determined for 120 vials located in the center of the shelf. Vial bottom curvature depth and contact area between the vial and the shelf were carefully measured for 120 vials and these data were used to calculate $K_v$ distribution due to variability in vial geometry. At low pressures commonly used for sensitive products (below 10 Pa), the vial-shelf contact area appeared crucial for explaining $K_v$ heterogeneity and was found to generate, in our study, a product temperature distribution of approximately 2 °C during sublimation. Our approach provides quantitative guidelines for defining vial geometry tolerance specifications and product temperature safety margins.

**Keywords:** Freeze drying/lyophilization; amorphous; drying; vaccines; distribution; vial heat transfer coefficient; sublimation rate; vial design; inter-vial heterogeneity

## INTRODUCTION

Nowadays, freeze-drying is an essential and valuable preservation method to ensure the long-term stability of the growing list of biopharmaceuticals such as antibodies, hormones, vaccines, therapeutics peptides and proteins. This method makes it possible to remove the majority of water at temperatures far below 0 °C (usually between -40 °C and -20 °C) by sublimation, the phase transition from ice to water vapor.[1]

Due to the really low temperature and pressure typically used, freeze-drying remains a time consuming process often difficult to control and scale-up. The US Food and Drug Administration has recently proposed a new regulatory philosophy to manage product quality: the Quality by Design (QbD) initiative. Quality will be no more tested into the product but designed into the process. The QbD approach is based on pre-defined quality targets and on a deep understanding of how formulations and process interact to influence critical quality attributes of pharmaceutical products.[2] In contrast to tablets, products intended to be freeze-dried are conditioned in their final packaging system (vial or syringe) before the process.[3] The vial thus directly influences the freeze-drying process and impacts final product quality.[4,5] Furthermore, since the capacity of a manufacturing freeze-dryer can easily reach 100 000 vials, ensuring uniform product quality attributes (potency of the active ingredient, residual moisture content, visual aspect of the freeze-dried cake) within the entire batch represents a real challenge. Any variation in the design of the packaging system or other parameters could result in product quality variation.

Product temperature is a key process parameter governing an important critical product quality attribute, the visual aspect of the freeze-dried cake, which in turn could influence the residual moisture, the stability of the active ingredient and the reconstitution time.[6] During the process the product temperature should be maintained below a critical value corresponding to the glass transition temperature in amorphous product.[3,7] However, the

product temperature profile cannot be directly controlled and depends on the process operating parameters (i.e., shelf temperature, chamber pressure) and on the heat transfer through the container (e.g., vial).[4,7,8] Knowledge of the heat transfer characteristics of the vial and the uniformity or non uniformity of this property within vial arrangement inside a freeze-dryer is thus essential to be able to predict final quality of the product batch. Several authors have reported that the heat transfer rate between the shelf and the product is dependent on the vial position on the shelf.[4,5,9–12] Pikal et al.[5] showed that the vials located at the periphery of the shelf exhibited sublimation rates 15% higher than vials located in the center. This phenomenon, referred to as "edge effect", has been ascribed to additional heat transfer by radiation from walls and doors.[4,5,8,9,11] The higher heat flow rate of these periphery vials could lead to product collapse due to increased product temperatures during the primary drying phase. Furthermore, Pisano et al.[10] recently observed a normal distribution in the vial heat transfer coefficient evaluated for vials located in the center of the shelf.

The design of the vial also strongly influences the heat transfer efficiency between the shelf and the product.[4,5,7,12–15] Considering that the vials are placed directly on the shelf, the heat flow transferred to the product can be described by three parallel mechanisms: conduction from the shelf surface to the vial *via* points of direct contact between the vial bottom and the shelf, conduction through the vapor entrapped in the vial bottom concavity and radiation.[5,8,12] Heat transfers *via* contact conduction and conduction through the gas are influenced, respectively, by the dimension of the contact area between the shelf and the vial and the depth of bottom curvature in which the gas is entrapped.[5,8,12] Several studies[13,16,17] have demonstrated that the vial bottom curvature limits the heat transfer and, thus, the sublimation flow rate that determines the duration of the primary drying. The concavity of the vial bottom limits the direct surface contact between the vial and the shelf, accounting for most of the resistance to conductive heat transfer.[14,16] In pharmaceutical freeze-drying conditions, contact

conduction is more efficient than gas conduction, and an increase in the contact area leads to a significant increase in the total heat transfer.[5,14]

Our objective was to quantitatively investigate the role of vial geometry distribution on heat transfer heterogeneity and subsequently on product quality by predicting product temperature distribution during the primary drying step induced by variability in vial dimensions. Proposing an approach to understand how vial design and operating conditions interact to influence product quality is completely in the scope of the QbD approach.

In the present study, only vials located in the center of the shelf and surrounded by other vials in the same conditions were considered so as to avoid any heterogeneity due to the additional border heat transfer. The analysis of the heterogeneity was conducted in terms of vial heat transfer coefficient ($K_v$) distributions. Based on theoretical analysis,[5,8,12] attention was focused on the role of two vial dimensions, the bottom curvature depth and the contact area between the bottom vial and the shelf. Two shelf temperatures (-40 °C and 0 °C) and six chamber pressures (4, 6, 9, 15, 40 and 50 Pa) were tested in two freeze-dryer pilot plants of similar shelf emissivity to assess the impact of these operative parameters on the heat transfer heterogeneity among central vials. Finally, as example of practical application of our work for assessing the pharmaceutical product quality, the impact of the central vial $K_v$ variability on product temperature was evaluated. Product temperature distributions for a 5 % sucrose solution were calculated from the simulated $K_v$ distributions based on the vial geometry for several operating conditions.

## MATERIALS AND METHODS

### Materials

Siliconized glass tubing vials (3 mL) were provided by Müller + Müller (Holzminden, Germany). These vials are routinely used in commercial manufacturing. Distilled water was used throughout the experiments.

Two pilot scale freeze-dryers differing mainly by their size, the type of valve connecting the drying chamber to the condenser and their age were used for this study:

- a LyoVac GT6 (Finn-Aqua Santasalo-Sohlberg SPRL, Brussels, Belgium), referred to as LYO A. It included 5 shelves with an area of 0.14 m² each, a distance between shelves of 56 mm, a drying chamber volume of 0.061 $m^3$ and a butterfly valve between the chamber and the condenser.
- an Epsilon 2-25D (Martin Christ Gefriertrocknungsanlagen GmbH, Osterode am Harz, Germany), referred to as LYO B. It included 7 shelves with an area of 0.27 m² each, a distance between shelves of 55 mm, a drying chamber volume of 0.38 $m^3$ and a mushroom valve between the chamber and the condenser.

The pressure in the freeze-dryer chamber was monitored by a capacitive manometer. Since it was not technically possible to install thermocouples in the drying chamber of the two freeze-dryers, Tempris wireless sensors (IQ Mobil Solution GMbH, Holzkirchen, Germany) were positioned in the bottom center of selected vials (Figure 1) to record ice temperature during the experiments. The obtained signal was used to define the sublimation starting point.

**Ice sublimation experiments**

All experiments were performed using a 1.8 mL fill volume of distilled water (filling height: 11 mm). No stopper was inserted into the vial neck. The middle shelf was fully covered by filled vials for all runs, corresponding to a total of 540 vials in LYO A and 950 vials in LYO B. Bottomless trays were used.

The vials were quickly loaded on the pre-cooled shelf at -50°C. The presence of a dry laminar flow in front of the freeze-dryer door made it possible to control the air relative humidity and thus to limit condensation on the shelves. After a freezing step of 2 hours, the pressure was decreased and the shelf temperature was increased by 1 °C/min. Experiments were carried out at 4, 6, 9, 15, 40 and 50 Pa with a shelf fluid inlet temperature of 0 °C, and at 4 and 6 Pa with a shelf fluid inlet temperature of -40 °C. The run performed at 0 °C and 6 Pa was repeated three times. The cycles were run long enough to dry up to 20-25 % of the initial fill volume. Subliming a larger quantity of ice could lead to loss of contact between the vial and the ice, introducing uncertainty in the analysis.

The sublimation rate $\dot{m}$ was measured gravimetrically for each vial and calculated as the mass loss divided by the period of sublimation. A total of 100 vials, placed in the centre of the shelf and surrounded by other vials in the same conditions, were individually weighed before and after the experiment on a precision scale (± 0.001 g; Mettler Toledo, Zaventem, Belgium). Sublimation time was measured from the moment when shelf temperature exceeded product temperature, meaning that there was a net heat flux from the shelf towards the vials. The arrangement of the weighed vials within the shelves is shown in Figure 1 for the two freeze-dryers.

**Measurement of emissivity of the vial and of the shelf**

Emissivity measurements were performed by Themacs Ingénierie (Champs sur Marne, France). The glass vial emissivity was determined using a Fourier transform infrared spectrophotometer (Frontier, Perkin Elmer, Roissy, France) equipped with a Pike© integrant sphere (Pike Technologies, Fitchburg, WI, USA). The measured emissivity varied from 0.78 to 0.80 within the range of temperatures tested (from -48 °C to 27 °C). Thus, a constant value

corresponding to the average observed product temperatures (between -48 to -24 °C) was used in the data analysis, as reported in Table 1.

The shelf emissivity was measured using the emissometer EM-2, making it possible an in situ measurement.[18] The emissivity value of the shelves of LYO B was 0.18 ± 0.06 (Table 1). Measurements were carried out on several pilot and production freeze-dryers and shelf emissivity values in the range of 0.18-0.3 were obtained. Considering the relative standard deviation of the method (0.06), the measured values are in agreement with values reported in literature.[5]

**Dimensional analysis of a batch of vials**

The dimensions of 120 vials were precisely measured by the specialized company Precis&Mans (Le Mans, France) using the micrometer Mitutoyo 3D (Mitutoyo Europe GmbH, Neuss, Germany). The following geometrical parameters were determined with a precision of 0.003 mm: the inner and outer bottom radius and the maximum bottom curvature depth. These values were used to calculate additional vial dimensions: outer and inner vial bottom area, vial shelf contact area ($A_c$) (named radius-based contact area in Table 1) and mean bottom curvature depth ($l$) (Appendix).

Furthermore, the vial-shelf contact area was also estimated using the imprint method proposed by Kuu et al.[17] and Hibler et al.[4] The vials were gently placed on an inkpad and then on a sheet of white paper. ImageJ v.1.49 software (National Institutes of Health, Bethesda, MD, USA) was used for the determination of the vial-shelf bottom contact area in pixels from the imprint images. The scale factor of pixels in $mm^2$ was determined by evaluating the number of pixels of a black shape of known area and was equal to 0.0153 $mm^2$ $pixel^{-1}$. The mean value and the relative standard deviation of these geometrical dimensions are reported in Table 1. The two methods used for evaluating the vial-shelf contact area gave similar mean

values: 16.7 mm² for the imprint method and 17.8 mm² for the dimensional analysis. However, the coefficient of variation of these methods appeared different and significantly higher for the imprint method (23.9 % versus 12.0 % for the dimensional analysis). The values of contact area determined using this latter method were selected for the analysis considering that this method better accounts for intimate contact between vial and shelf.

## THEORY AND DATA ANALYSIS

### Evaluation of the vial heat transfer coefficient $K_v$ based on experimental data

As widely reported in literature,[4,5,8,12] the vial heat transfer coefficient $K_v$ was calculated using the following equation:

$$K_v = \frac{\dot{Q}}{A_b(T_s - T_b)} = \frac{\Delta H\, \dot{m}}{A_b(T_s - T_b)} \qquad \text{Equation 1}$$

where $\dot{Q}$ is the heat flow received by the vial, $A_b$ is the outer vial bottom area, $T_s$ is the average temperature between the inlet and outlet shelf fluid temperatures, $T_b$ is the bottom product temperature, $\Delta H$ is the latent heat of sublimation and $\dot{m}$ is the sublimation rate.

Since it was not possible to implement thermocouples in the freeze-dryer pilot plant to have a precise measurement of the product temperature, $T_b$ was theoretically determined as:

$$\dot{Q} = \frac{\lambda_{ice}}{L_{ice}} A_{in}(T_b - T_i) \qquad \text{Equation 2}$$

where $\lambda_{ice}$ is the ice thermal conductivity, $A_{in}$ is the inner bottom area of the vial, $L_{ice}$ is the ice thickness and $T_i$ is the ice-vapor interface temperature. The ice thickness was estimated as

the mean between the initial and final ice thickness values (calculated using the amounts of initial and sublimed ice).

No stopper and pure water were used in this study in order to assume that the partial pressure of vapor at the sublimation interface was equal to the chamber pressure. The temperature at the ice-vapor interface $T_i$ was thus calculated as a function of the interface pressure $P_i$ using the Clausius-Clapeyron relation:[19]

$$T_i = \frac{6139.6}{28.8912 - \ln(P_i)} \qquad \text{Equation 3}$$

The $T_b$ value calculated was compared to the product temperature value given by the Tempris probe and an excellent agreement between experimental and theoretical data was observed.

**Theoretical description of the vial heat transfer coefficient $K_v$**

The main objective of this work was to quantify the impact of vial dimensions distribution on heat transfer variability and its resulting consequence on product temperature. To this end, the vial heat transfer coefficient need to be theoretically expressed in function of specific vial dimensions.

The vial heat transfer coefficient $K_v$ can be described as the sum of three contributions:[5,8,12]

$$K_v = K_c + K_g + K_r \qquad \text{Equation 4}$$

where $K_c$ represents the thermal contact conduction between the shelf and the vial *via* the direct contact area, $K_g$ the thermal conduction through the gas entrapped in the vial bottom curvature and $K_r$ the thermal radiation between the vial and the top and bottom shelves.

*Heat transfer by thermal contact conduction $K_c$*

The expression of $K_c$ has been discussed in the literature by only a few authors.[16,17] Kuu et al.[17] proposed an evaluation of this parameter and showed that the larger the contact area is, the larger the value of the contact conduction coefficient will be. Thus, $K_c$ can be assumed to be proportional to the contact area ($A_c$, evaluated by the imprint test method) through an empirical constant ($C_1$):

$$K_c = C_1 \, A_c \qquad \text{Equation 5}$$

*Heat transfer by conduction through the gas $K_g$*

The coefficient $K_g$, representing the contribution of the conduction through the gas in $K_v$, can be expressed as:[5,12]

$$K_g = \frac{C_2 \, P_C}{1 + \frac{C_2 \, l}{\lambda_{amb}} P_C} \qquad \text{Equation 6}$$

where $P_C$ is the chamber pressure, $\lambda_{amb}$ is the molecular conductivity of the water vapor at ambient pressure, $l$ is the mean vial bottom curvature depth calculated as reported in the Appendix, and the coefficient $C_2$ is equal to:

$$C_2 = \Lambda_o \frac{\alpha_c}{2 - \alpha_c} \left( \frac{273.15}{T_{gas}} \right)^{0.5} \qquad \text{Equation 7}$$

where $\Lambda_o$ is the free molecular heat conductivity of the gas at 0 °C, $T_{gas}$ is temperature of the gas participating to heat conduction, calculated as average between the product temperature

at the sublimation interface and the shelf temperature values,[12] and $\alpha_c$ is the accommodation coefficient.

*Heat transfer by thermal radiation $K_r$*

The heat transfer by radiation between the shelf and the vial $\dot{Q}_r^{shelf}$ can be described by the Stephen-Boltzmann equation:[5,8,20]

$$\dot{Q}_r^{shelf} = A_r\, \mathcal{F}\, \sigma\, ({T_s}^4 - {T_b}^4) \qquad \text{Equation 8}$$

where $A_r$ is the area exposed to the radiation from the shelves to be considered equal to the vial bottom area $A_b$, $\mathcal{F}$ is the visualization factor and $\sigma$ the Stephan-Boltzman constant. After mathematical rearrangement, Equation 8 can be expressed as:

$$\dot{Q}_r^{shelf} = A_r\, \mathcal{F}\, \sigma\, \left({T_s}^4 - {T_b}^4\right) = A_b\, \mathcal{F}\, \sigma (T_s + T_b)(T_s^2 + T_b^2)(T_s - T_b) \qquad \text{Equation 9}$$

Thus, the heat transfer coefficient $K_r$ for thermal radiation can be defined as:

$$K_r = \mathcal{F}\, \sigma\, (T_s + T_b)(T_s^2 + T_b^2) \qquad \text{Equation 10}$$

During the process, central vials are affected by two different radiative heat transfer contributions: between (i) the shelf below the vial and the vial bottom, and (ii) the shelf above the vial and the top of the vial.[5,8,12] Hence, the visualization factor will be the sum of two terms:

$$\mathcal{F} = \mathcal{F}_b + \mathcal{F}_{top} \qquad \text{Equation 11}$$

The visualization factor at the bottom of the vial $\mathcal{F}_b$ can be evaluated considering the definition proposed by Bird et al.[20] and Pikal[8] for the heat transfer by radiation between parallel surfaces:

$$\mathcal{F}_b = \frac{1}{1+\left(\frac{1}{e_v}-1\right)+\left(\frac{1}{e_s}-1\right)} \qquad \text{Equation 12}$$

where $e_v$ and $e_s$ are the emissivities of the vial and shelf, respectively.

Considering vials located in the centre of the shelf and surrounded by other vials in the same conditions, it is possible to assume that (i) the vial area exposed to the top shelf is much smaller than the area of the shelf and (ii) the vial top does not receive radiations from the side walls of the chamber. Thus, the visualization factor between the top of the vials and the shelf $\mathcal{F}_{top}$ can be estimated equal to the emissivity of the vial:[5,8]

$$\mathcal{F}_{top} = e_v \qquad \text{Equation 13}$$

In agreement with the literature, the visualization factor at the vial top (equal to 0.78; Table 1) is higher than the one at the vial bottom (equal to 0.16; Table 1).[5]

*Dependence of the vial heat transfer coefficient on vial geometry*

Equations 4, 5 and 6 were combined to highlight the dependence of $K_v$ on the contact area ($A_c$), and bottom curvature depth ($l$):

$$K_v = C_1\, A_c + K_r + \frac{C_2\, P_c}{1+\frac{l}{\lambda_{amb}}\, C_2\, P_c} \qquad \text{Equation 14}$$

The term $K_r$ was calculated from Equations 10-13 for each experimental condition. Coefficients $C_1$ and $C_2$ were determined by fitting Equation 14 in a least-squares sense to experimental $K_v$ values determined by the gravimetric method. Calculations were performed with Matlab R2014b software equipped with the Statistics Toolbox (The Mathworks Inc., Natick, MA, USA). The bottom curvature depth $l$ and contact area $A_c$ were evaluated from dimensional analysis of the vial and imprint test, respectively.

**Calculation of $K_v$ distributions based on vial geometry**

Two vial dimensions influence heat transfer: the contact area ($A_c$) and the mean bottom curvature depth ($l$). The absence of correlation between the two geometrical dimensions $l$ and $A_c$ was verified by calculating the correlation factor together with its statistical significance (p-value > 0.5). It was thus possible to independently evaluate the impact of those parameters on $K_v$. Using Equation 14, three $K_v$ distributions based on vial dimension variations were simulated: (i) curvature-based ($l$ in Equation 14); (ii) contact area-based ($A_c$ in Equation 14); and (iii) their combination. The curvature-based $K_v$ distribution was obtained by evaluating Equation 14 with the 120 measured values of the mean bottom curvature depth ($l$), while the contact area was maintained constant at its mean value. The contact area-based $K_v$ distribution was obtained by evaluating Equation 14 with the 120 measured values of the imprint-based contact area ($A_c$), whereas the bottom curvature depth was maintained constant at its mean value. Plugging both measured $l$ and $A_c$ values into Equation 14 gave the combined contact area and curvature-based $K_v$ distribution. The calculation was repeated for all the studied chamber pressures and shelf temperatures. Chi-square goodness-of-fit tests were performed on the simulated $K_v$ distributions, establishing that the sample data were consistent with a normal distribution at a 0.05 significance level.

324 **Simulation of the product temperature distributions using the $K_v$ distribution**

325 Product temperature distributions were obtained from the calculated contact area and
326 curvature-based $K_v$ distribution. The product temperature was calculated for a 5 % w/w
327 sucrose solution, considering a shelf temperature of -25°C and four chamber pressures (4, 6,
328 9, 15 Pa). Pressure at 40 and 50 Pa were not considered because the product temperature
329 exceeds the glass transition temperature of the product at such high pressure (i.e., -32 °C for a
330 5 % w/w sucrose solution).[21] In the case of a real product, the mass flow rate can be
331 expressed as reported by Pikal et al.[5]:

332

333 $$\dot{m} = \frac{(P_i - P_c)\, A_{in}}{R_p} \qquad \text{Equation 15}$$

334

335 where $R_p$ represents the area-normalized product resistance. The value of $R_p$ used for this
336 simulation is reported in Table 1 and was considered for a dried layer thickness of 0.5 cm.[21]
337 To simulate the product temperature distribution, the non-linear system composed of
338 Equations 1-3 and 14-15 was solved for each pair of measured $l$ and $A_c$ values. Chi-square
339 goodness-of-fit tests were performed on the product temperature distributions, demonstrating
340 that the simulated data were compatible with a normal distribution at a 0.05 significance
341 level.

342

343 **RESULTS AND DISCUSSION**

344 **Impact of equipment on $K_v$**

345 Vial heat transfer coefficient $K_v$ of 100 vials located in the centre of the shelf was
346 experimentally determined for different chamber pressures (4 to 50 Pa), shelf temperatures (-
347 40 °C and 0 °C) and freeze-dryers (LYO A and LYO B). Figure 2 illustrates the evolution of
348 the average value of $K_v$ with pressure. Equation 14 was fitted with the experimental data and

349 the resulting coefficients $C_1$ and $C_2$ are presented in Table 2 for the data obtained in LYO A,
350 LYO B and their combination. The accommodation coefficient $\alpha_c$ was also calculated from
351 Equation 7, considering an average value of the gas temperature obtained under the different
352 operating conditions tested ($T_{gas}$ = -35 °C). The obtained values of the accommodation
353 coefficient appear to be in agreement with data in literature.[8]
354 In Table 2, LYO A and LYO B exhibited a similar value of the $C_1$ coefficient that is related
355 to the contact area coefficient $K_c$ (Equation 5), but distinct values of the $C_2$ coefficient that is
356 related to $K_g$ (Equation 6). LYO B exhibited a slightly higher accommodation coefficient
357 then LYO A, probably due to a different finish of the freeze-dryer shelf material.
358 When considering pressure values lower than 10 Pa (Figure 2), the $K_v$ values obtained in the
359 two freeze-dryer appeared similar. This result was confirmed also by Pisano,[12] who reported
360 no significant difference in $K_v$ value of central vials processed in a pilot and manufacturing
361 freeze-dryer at a pressure of 10 Pa. For pressure value higher than 10 Pa, the influence of
362 freeze-dryer configuration became significant with slightly higher values obtained in LYO B
363 (Figure 2). At 50 Pa, the $K_v$ value was approximately 8% higher in LYO B than in LYO A.
364 Considering the different values of $C_2$ coefficient, the $K_v$ difference between freeze-dryers at
365 high pressure can thus be ascribed to the increased rate of heat transfer through the gas over
366 the total heat flow. However, the physical origin of the differences in the pressure-dependent
367 component of $K_v$ remains unclear. Possible hypotheses include: (i) differences in the shelf
368 surface finish that could induce differences in the gas-shelf heat transfer through the
369 accommodation coefficient[8] (Equation 6-7) as well as (ii) differences in the gas convection
370 conditions, a mechanism responsible for a small part of the pressure-dependent heat
371 transfer.[22] These results suggest that small differences between devices might become more
372 apparent at high pressures. When considering only vials not exposed to edge effect a cycle
373 designed with low operating pressure (below 10 Pa) could therefore be more suitable for safe

374 scale-up. However the behavior of the edge vials located at the periphery of the shelf or in
375 contact with metallic band need also to be considered and some elements were recently
376 proposed by Pikal et al.[11] to investigate the impact of the freeze-dryer configuration.
377

378 **Impact of chamber pressure and shelf temperature on $K_v$**

379 As reported in the literature and shown in Figure 2, chamber pressure had a strong impact on
380 $K_v$.[4,5,8,12,13,15] The vial heat transfer coefficient increased approximately four times between 4
381 and 50 Pa. At the vial bottom, the presence of the curvature limits the intimate contact
382 between the shelf and the vial and create an empty space between the shelf and the vial that
383 acts as an insulator.[13,16,17] At very low pressures typically used in the process, the heat
384 transfer contribution by gas convection is usually neglected,[11] whereas the contribution of gas
385 conduction has to be considered. This heat transfer mechanism, represented by the coefficient
386 $K_g$, is dependent on the chamber pressure and increases when increasing pressure, as shown
387 in Equation 6.[5,8,12,15] Figure 3 shows the relative contributions of $K_c$, $K_r$ and $K_g$ on the total
388 $K_v$, calculated using the set C of the fitting coefficients reported in Table 2. The $K_c$ and $K_r$
389 contributions go from about 30 % at 4 Pa to 10 % at 50 Pa, whereas the $K_g$ contribution goes
390 from about 25 % at 4 Pa to 80 % at 50 Pa.

391 A moderate effect of shelf temperature on $K_v$ was expected theoretically due to $K_r$ (Equation
392 10) and to $K_g$ through the gas temperature (Equations 6-7). Figure 4a displays the influence
393 of shelf temperature on $K_v$. Differences in $K_v$ values due to temperature remained within the
394 standard deviation when considering pressure values lower than 10 Pa and when the
395 contribution of $K_g$ in the total $K_v$ is moderate (around 25 %, Figure 3).

396 In order to clarify the impact of the shelf temperature, the contributions of the single
397 coefficients $K_c$, $K_r$ and $K_g$ on $K_v$ were calculated for two shelf temperatures (25 °C and -25
398 °C) and three chamber pressures (4, 6 and 50 Pa), as show in Figure 4b. The contact

399 conduction coefficient $K_c$ does not depend on the shelf temperature (Equation 5) and thus has
400 a constant contribution in $K_v$ for all the temperatures tested. The radiative coefficient $K_r$
401 depends on the third power of the shelf temperature and increases by about 1 $W\ m^{-2}\ K^{-1}$
402 between -25 °C and 25 °C for all pressures considered. The gas conduction coefficient $K_g$
403 depends on the gas temperature and decreases by 0.1-0.2 $W\ m^{-2}\ K^{-1}$ at low pressures (4-6
404 Pa) and by 1.1 $W\ m^{-2}\ K^{-1}$ at 50 Pa, between the two considered values of shelf temperature.
405 When increasing shelf temperature, the increase of $K_r$ is partly compensated by the decrease
406 of $K_g$. These results confirm that the dependence of $K_v$ on the shelf temperature is negligible,
407 especially if compared with the role played by the chamber pressure. Pisano et al.[12] and
408 Hottot et al.[23] reported similar $K_v$ values for different shelf temperature conditions.
409
410 **Inter-vial heat transfer heterogeneity and the role of vial dimensions**
411 Figure 5 presents the experimentally observed distributions of the vial heat transfer
412 coefficient data of central vials at six chamber pressures. Since temperature- and equipment-
413 induced variations were minor, data obtained in LYO A and B and for the two shelf
414 temperatures were merged. A significant variability in the $K_v$ values evaluated for central
415 vials was observed, the standard deviation increasing with pressure from 0.84 to
416 2.46 $W\ m^{-2}\ K^{-1}$. The values of standard deviation corresponded to coefficient of variation
417 comprised between 4 and 8 % depending on the operating conditions. The measurement error
418 associated to the determination of $K_v$ was evaluated as the sum of the individual
419 measurement accuracy of each parameter entering in the calculation of $K_v$ (Equation 1). The
420 measurement uncertainty was estimated to be ~ 1 %. This value is in agreement with the
421 value reported by Pikal et al.[5], who reported an uncertainty value of ~1.2 %. The
422 measurement uncertainty alone did not allow to completely explain the variability of the $K_v$

423 data. An external factor responsible for inter-vial heat transfer heterogeneity had thus to be
424 considered.
425 Attention was focused on the container: the geometrical difference among the vials was
426 considered as a possible source of the heat transfer heterogeneity. This variability in the vial
427 dimensions can be due to production limits and could change as a function of the container
428 model and provider. For the tested vial set, the coefficient of variation was approximately
429 27.7 % for the mean bottom curvature depth ($l$) and 23.9 % for the imprint-based contact area
430 ($A_c$). Hence, the effect of the variability of these geometrical dimensions on $K_v$ was evaluated
431 as proposed in the Theory and data analysis section using the set of coefficients C reported in
432 Table 2.
433 Figure 6 displays the simulated distributions of $K_v$ based on the vial bottom dimensions.
434 These distributions showed a trend and range of $K_v$ values similar to the experimental ones.
435 At low pressure, $K_v$ variability is almost completely due to the contact area variability. The
436 importance of the contact area on the $K_v$ value was also confirmed by Pikal et al.[5] and
437 Cannon et al.[16] Regarding the vial bottom curvature, the importance of its variability
438 increased when the pressure rose. This is due to the coefficient $K_g$ that plays a major role in
439 the total value of $K_v$ at 40 and 50 Pa, as shown in Figure 3. The role of the bottom curvature
440 dimension was previously investigated by Brülls and Radsmuson[15] and Cannon et al.[16] Brülls
441 and Radsmuson[15] have shown that the bottom curvature has an impact on the heat transfer
442 only at chamber pressures higher than 30 Pa. This conclusion was confirmed by Cannon et
443 al.[16], who found that bottom curvature had little impact when considering low pressure (< 27
444 Pa). Our results agree with these conclusions,[15,16] confirming that the variability of the
445 bottom curvature depth has to be taken into consideration only if cycles at high chamber
446 pressure are performed (> 30 Pa).

Figure 7 displays the coefficient of variation of the experimental and calculated $K_v$ distributions at different pressures. For the experimental distributions, the coefficient was calculated as an average between the LYO A and B datasets. The trend of the observed coefficient of variations for both experimental and simulated $K_v$ distributions decreased from approximately 9 % to 4 % when increasing the chamber pressure. The variability of the experimental $K_v$ distributions is completely explained by the geometrical variability at low pressures (i.e., 4, 6 Pa), whereas at higher pressures, the experimental coefficient of variation appears to be slightly higher than the one calculated based on vial geometry. It is thus possible that other sources of variability should be taken into consideration, for example convection in the drying chamber could play a role if higher pressures are considered.[22]

These considerations can guide the selection of the container as a function of the variability of the vial dimensions. The results obtained show that at low chamber pressure (i.e., 4, 6, 9, 15 Pa), it is important to assess the variability of the contact area between the vial and the shelf, whereas for cycles performed at high pressure (i.e., 40, 50 Pa), the variability of the bottom curvature depth becomes a relevant parameter. Consequently, for pharmaceutical processes that are usually carried out at pressures lower than 10 Pa, the contact area needs to be taken into account more than the bottom curvature depth.

**Impact of $K_v$ heterogeneity on the product temperature distribution within a batch of vials located in the centre of the shelf and not exposed to edge effect**

In the case of freeze-drying, product temperature is one of the most important critical quality parameters. During the process, product temperature must be maintained close to a limit value (i.e., glass transition temperature for amorphous products, $T_g$) in order to optimize the process time but not to exceed it so as to guarantee the visual aspect of the cake and the product quality.

The vial-to-vial heat and mass transfer heterogeneity during the sublimation step causes variability in the product temperature. Considering a constant and fixed value of mass transfer resistance, it would be interesting to estimate the product temperature distribution during the primary drying step resulting only from the variability in vial geometry. Product temperature distributions were thus evaluated considering the contact area and curvature-based $K_v$ distributions. For this analysis, a 5 % w/w sucrose solution was considered, processed at -25 °C and four different pressures (4, 6, 9 and 15 Pa). Relevant data concerning product resistance and glass transition temperature (-32 °C) were found in the literature.[21] As expected, product temperature increased from 4 Pa to 15 Pa because of the higher value of the vial heat transfer coefficient and higher ice sublimation temperature.

The variability of the product temperature was estimated to be approximately 0.9 °C at 15 Pa and as large as 2.2 °C at 4 Pa, considering ± 3 times the standard deviation that includes 99 % of the vials (Figure 8). A practical implication of these results is that, at the low pressures commonly encountered in vaccine freeze-drying, a temperature safety margin of approximately 2 °C has to be considered with respect to cycles designed on the basis of an average $K_v$ value and to vials not exposed to edge effect.

Vials located at the periphery of the shelf (i.e., edge vials) receive additional heating due to the radiation from the chamber walls and the contact with the metallic guardrail. Thus, edge vials present a higher sublimation rate and a higher product temperature respect central vials.[5] Tang et al.[24] reports that the temperature difference between edge vials and central vial can be up to 2 °C at a shelf temperature of 20 °C and up to 4 °C at -30 °C for a chamber pressure of about 10 Pa. Depending on the operating conditions of the process, the safety product temperature margin resulting from variability in vial dimensions could be in the same order of magnitude than the safety margin imposed by the "edge effect".

## CONCLUSIONS

Implementation of the Quality by Design initiative require a precise definition of the acceptable range for all product and process variables ensuring the fulfillment of the critical quality attributes of the final product. The impact of any variation of these variables on the final quality need to be quantified in advance. In this work, the effect of the variability of geometrical dimensions observed within a batch of vials (i.e., contact area between the shelf and the vial and the mean bottom curvature depth) on product quality was explored. The product quality was evaluating by predicting the product temperature knowing the vial heat transfer coefficient $K_v$. An original approach was proposed to calculate $K_v$ distribution based on geometrical dimensions when considering a batch of vials located in the center of the shelf not exposed to any edge effect. The impact of freeze-dryer configuration and operating conditions was also considered. When considering low pressure (< 10 Pa), commonly used for freeze-drying biopharmaceuticals, the influence of freeze-dryer configuration and shelf temperature on heat transfer characteristics can be neglected and $K_v$ distribution is completely explained by the contact area distribution. Furthermore the variability of vial dimension results in the definition of a product temperature safety margin of 2 °C. However, additional sources of variability need to be included in QbD approach. In particular, a study focused on the variability between edge and central vials and its role in cycle scale-up is presently ongoing.

## ACKNOWLEDGMENTS

The authors would like to thank Benoit Moreau and Yves Mayeresse (GSK Vaccines) for reviewing this manuscript and Vincent Ronsse (technician) and Alain Philippart (operator) (GSK Vaccines) for their help in the data acquisition.

## CONFLICT OF INTEREST

Erwan Bourlés is an employee of the GSK group of companies. Bernadette Scutellà participated in a postgraduate PhD program at GSK Vaccines. Stephanie Passot, Fernanda Fonseca and Ioan Cristian Trelea report no financial conflicts of interest.


## FUNDING

This work was funded by GlaxoSmithKline Biologicals S.A., under a Cooperative Research and Development Agreement with INRA (Institut National de la Recherche Agronomique) via the intermediary of the UMR (Unité Mixte de Recherche) GMPA (Génie et Microbiologie des Procédés Alimentaires) at the INRA Versailles-Grignon research center.


## AUTHORS' CONTRIBUTIONS

Bernadette Scutellà, Stephanie Passot, Erwan Bourlés, Fernanda Fonseca and Ioan Cristian Trelea were involved in the conception and design of the study. Bernadette Scutellà and Erwan Bourlès acquired the data. Bernadette Scutellà, Stephanie Passot, Erwan Bourlès, Fernanda Fonseca and Ioan Cristian Trelea analyzed and interpreted the results. All authors were involved in drafting the manuscript or revising it critically for important intellectual content. All authors had full access to the data and approved the manuscript before it was submitted by the corresponding author.

## APPENDIX

The evaluation of the mean bottom curvature depth $l$ was performed from geometrical considerations on the semi-spherical calotte at the vial bottom, as represented in Figure A. The bottom curvature depth depends on the radius of the vial bottom as follows:

$$l(r) = R_c - a(r) \qquad \text{Equation A1}$$

where $R_c$ is the radius of the calotte and $a(r)$ is the distance between the shelf and the vial bottom, measured normal to the vial bottom:

$$a(r) = \sqrt{(R_c - l_{max})^2 + r^2} \qquad \text{Equation A2}$$

$R_c$ can be calculated as a function of the maximum bottom curvature depth $l_{max}$ and the inner vial bottom radius $R_i$:

$$R_c^2 = R_i^2 + (R_c - l_{max})^2 \qquad \text{Equation A3}$$

The area-mean bottom curvature depth can be defined as the integral of $l(r)$ on the calotte, divided by the area:

$$l = \frac{1}{A} \int l(r)\, dA \qquad \text{Equation A4}$$

The relevant area for heat transfer by gas conduction is:

$$A = \pi\, R_i^2 \qquad \text{Equation A5}$$

and the area element:

$$dA = 2\pi\, rdr \qquad \text{Equation A6}$$

Combining Equations A1-A6, $l$ was calculated as:

$$l = \frac{2}{R_i^2}\int_0^{R_i}(R_c - \sqrt{(R_c - l_{max})^2 + r^2}\,)\, r\, dr \qquad \text{Equation A7}$$

576 **REFERENCES**


577 1. Jennings TA. 1999. Lyophilization: introduction and basic principles. Englewood, CO:
578 Interpharm Press.
579 2. Nail SL, Searles JA. 2008. Elements of quality by design in development and scale-up of
580 freeze parenterals. Biopharm Int 21(1):44–52.
581 3. Franks F. 1998. Freeze-drying of bioproducts: putting principles into practice. Eur J
582 Pharm Biopharm 45:221–229.
583 4. Hibler S, Wagner C, Gieseler H. 2012. Vial Freeze-Drying, part 1: New Insights into
584 Heat Transfer Characteristics of Tubing and Molded Vials. J Pharm Sci 101(3):1189–
585 1201.
586 5. Pikal MJ, Roy ML, Shah S. 1984. Mass and heat transfer in vial freeze-drying of
587 pharmaceuticals: role of the vial. J Pharm Sci 73(9):1224–1237.
588 6. Johnson R, Lewis L. 2011. Freeze-drying protein formulations above their collapse
589 temperatures: possible issues and concerns. Am Pharm Rev 14(3):50–54.
590 7. Hibler S, Gieseler H. 2012. Heat transfer characteristics of current primary packaging
591 systems for pharmaceutical freeze-drying. J Pharm Sci 101(11):4025–4031.
592 8. Pikal MJ. 2000. Heat and mass transfer in low pressure gases: applications to freeze
593 drying. In Drugs and the Pharmaceutical Sciences 102:611–686.
594 9. Rambhatla S, Pikal MJ. 2003. Heat and mass transfer scale-up issues during freeze-
595 drying, I: atypical radiation and the edge vial effect. Aaps Pharmscitech 4(2):22–31.
596 10. Pisano R, Fissore D, Barresi AA, Brayard P, Chouvenc P, Woinet B. 2013. Quality by
597 design: optimization of a freeze-drying cycle via design space in case of heterogeneous
598 drying behavior and influence of the freezing protocol. Pharm Dev Technol 18(1):280–
599 295.

600 11. Pikal MJ, Bogner R, Mudhivarthi V, Sharma P, Sane P. 2016. Freeze-Drying Process
601 Development and Scale-Up: Scale-Up of Edge Vial Versus Center Vial Heat Transfer
602 Coefficients, Kv. J Pharm Sci doi:10.1016/j.xphs.2016.07.027.
603 12. Pisano R, Fissore D, Barresi AA. 2011. Heat Transfer in Freeze-Drying Apparatus. In:
604 Dos Santos Bernardes MA ed., Developments in Heat Transfer 91-114. Rijeka, Croatia:
605 InTech. Available from: http://www.intechopen.com/books/developments-in-heat-
606 transfer/heat-transfer-infreeze-drying-apparatus.
607 13. Nail SL. 1980. The Effect of Chamber Pressure on Heat Transfer in the Freeze Drying of
608 Parenteral Solutions. PDA J Pharm Sci Technol 34(5):358–368.
609 14. Ybema H, Kolkman-Roodbeen L, te Booy MP, Vromans H. 1995. Vial lyophilization:
610 calculations on rate limitation during primary drying. Pharm Res 12(9):1260–1263.
611 15. Brülls M, Rasmuson A. 2002. Heat transfer in vial lyophilization. Int J Pharm 246(1-
612 2):1–16.
613 16. Cannon A, Shemeley K. 2004. Statistical evaluation of vial design features that influence
614 sublimation rates during primary drying. Pharm Res 21(3):536–542.
615 17. Kuu WY, Nail SL, Sacha G. 2009. Rapid determination of vial heat transfer parameters
616 using tunable diode laser absorption spectroscopy (TDLAS) in response to step-changes
617 in pressure set-point during freeze-drying. J Pharm Sci 98(3):1136–1154.
618 18. Monchau JP, Marchetti M, Ibos L, Dumoulin J, Feuillet V, Candau Y. 2014. Infrared
619 Emissivity Measurements of Building and Civil Engineering Materials: A New Device
620 for Measuring Emissivity. Int J Thermophys 35:1817-31.
621 19. Trelea IC, Passot S, Fonseca F, Marin M. 2007. An Interactive Tool for the Optimization
622 of Freeze-Drying Cycles Based on Quality Criteria. Dry Technol 25(5):741–751.
623 20. Bird RB, Stewart WE, Lightfoot EN. 1960. Transport phenomena. New York, NY: John
624 Wiley & Sons.

21. Konstantinidis AK, Kuu W, Otten L, Nail SL, Sever RR. 2011. Controlled nucleation in freeze -drying: Effec and primary drying rate. J Pharm Sci 100(8):3453–3470.
22. Ganguly A, Nail SL, Alexeenko A. 2013. Experimental Determination of the Key Heat Transfer Mechanisms in Pharmaceutical Freeze-Drying. J Pharm Sci 102(5):1610–1625.
23. Hottot A, Vessot S, Andrieu J. 2005. Determination of mass and heat transfer parameters during freeze-drying cycles of pharmaceutical products. PDA J Pharm Sci Technol 59(2): 138–153.
24. Tang X, Nail SL, Pikal MJ. 2006. Evaluation of manometric temperature measurement, a process analytical technology tool for freeze-drying: Part I, product temperature measurement. AAPS PharmSciTech 7(1):E95–E103.

638 **FIGURES**

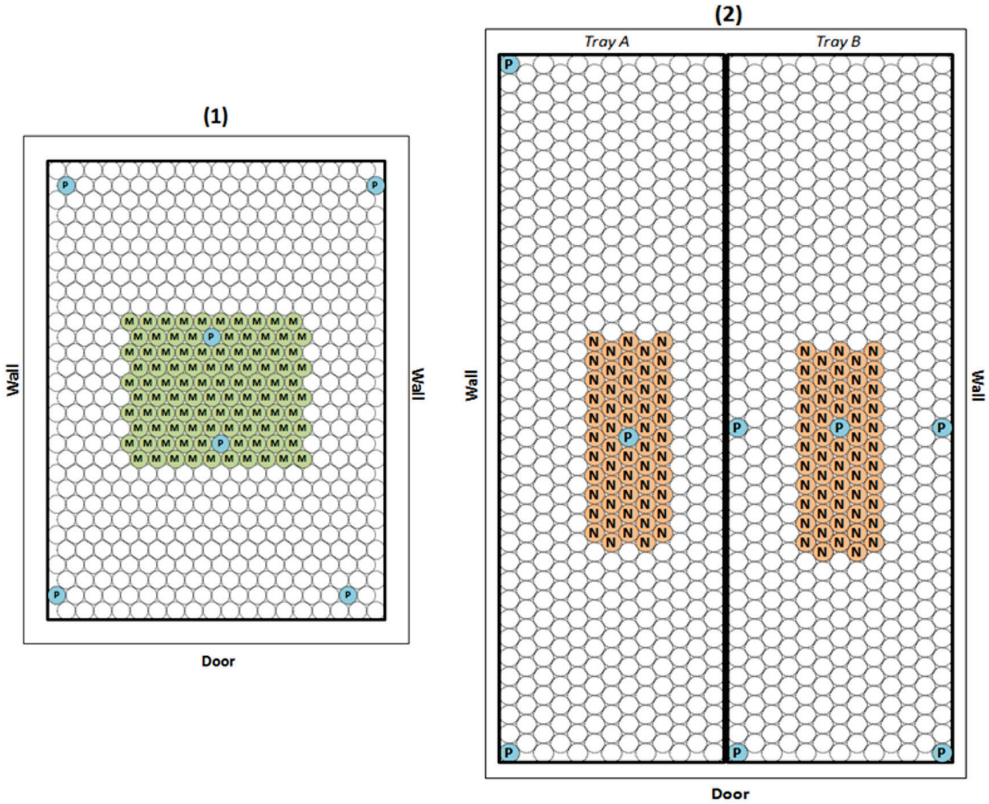


639

640 **Figure 1.** Vial arrangements in (1) LYO A and (2) LYO B. Gravimetrically-analyzed vials
641 are marked with the letters M and N for LYO A and B, respectively. Vials in which wireless
642 temperature probes were located are marked with the letter P. All vials were filled with 1.8
643 mL of pure water.

644

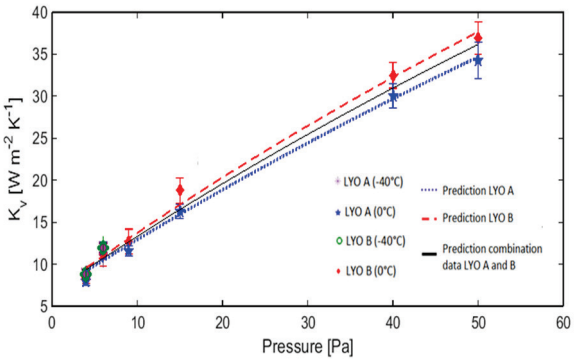


645

**Figure 2.** Vial heat transfer coefficient ($K_v$) values vs. chamber pressure ($P_c$). The markers refer to the $K_v$ average values measured in LYO A and B at -40°C and 0°C. The lines correspond to the values calculated with Equation 14 with the data obtained from LYO A, B and their combination. Error bars represent standard deviations.

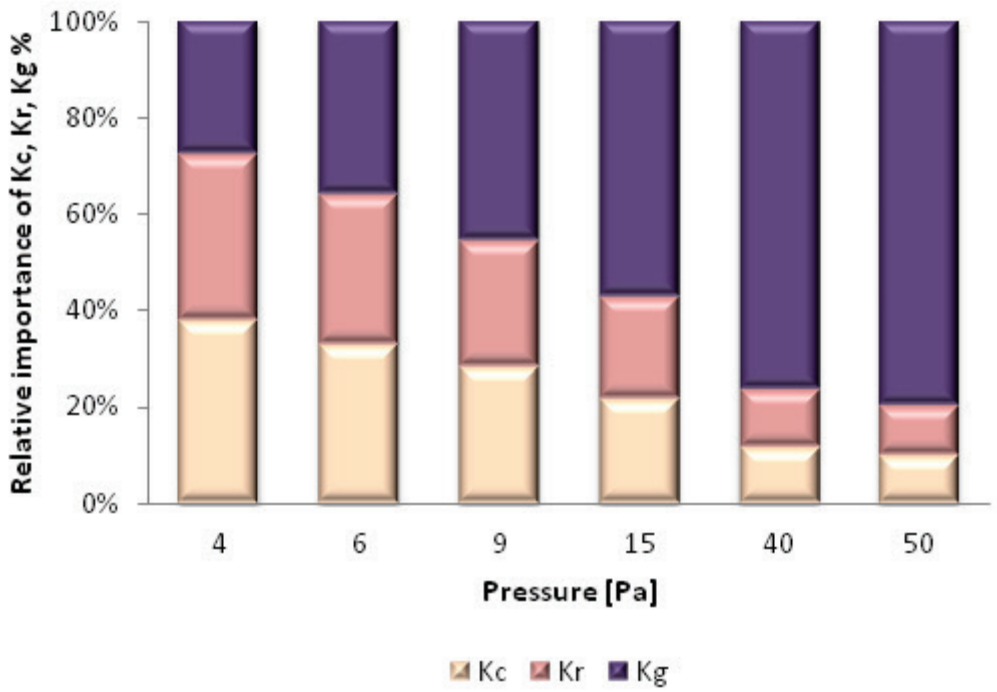


**Figure 3.** Relative importance of the heat transfer coefficients by contact conduction ($K_c$), radiation ($K_r$) and conduction through the gas ($K_g$) as percentages of the total heat transfer coefficients ($K_v$). Average values of the contact area ($A_c$) and mean bottom curvature depth ($l$) were considered in this calculation. The set of coefficients C (Table 2) was used to evaluate $K_c$ and $K_g$.

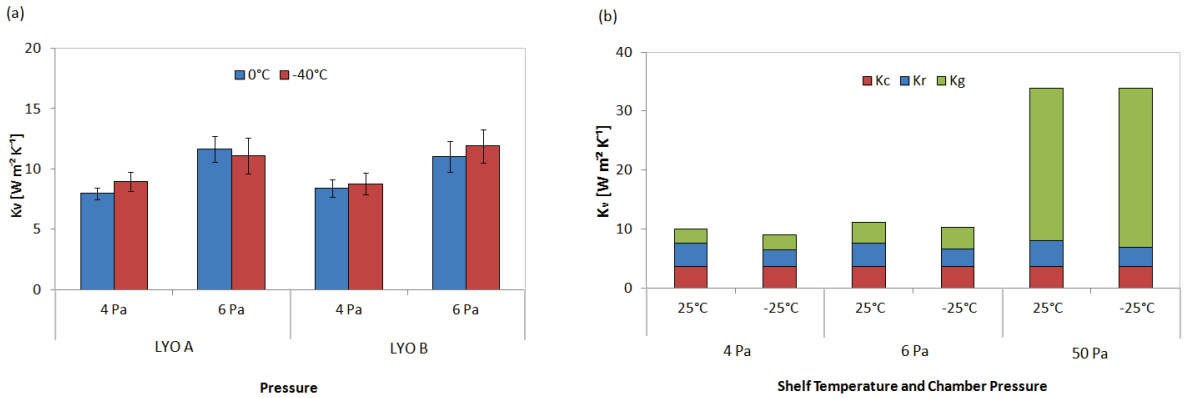


**Figure 4.** Influence of the shelf temperature on the vial heat transfer coefficients $K_v$. $K_v$ values were evaluated at different shelf temperatures and chamber pressures (a) from experimental data obtained in LYO A and B and (b) from the coefficients $K_c$, $K_r$ and $K_g$, calculated using Equations 5, 6 and 10.

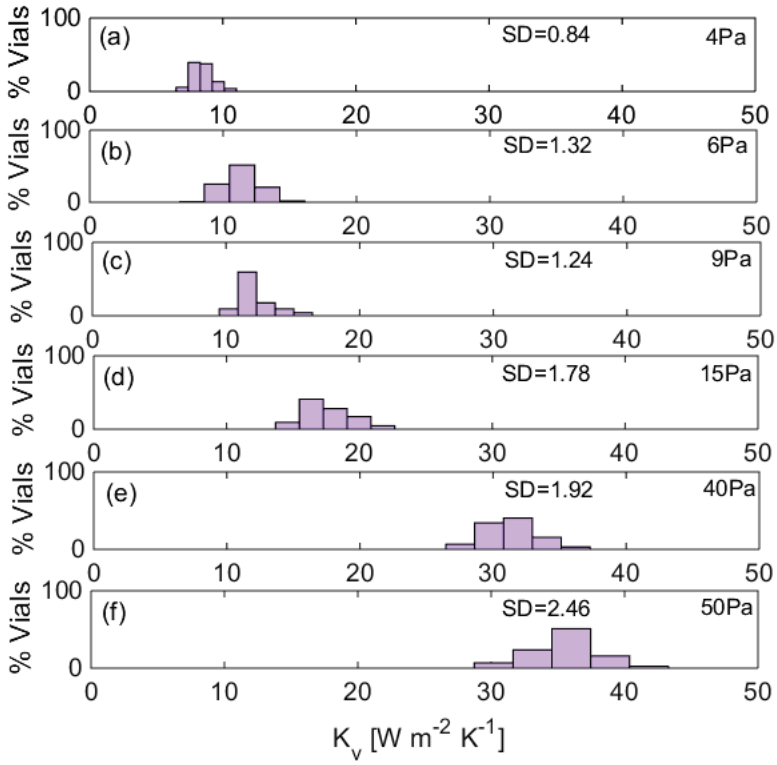


**Figure 5.** Experimentally-measured distribution of the vial heat transfer coefficients at 4 Pa (a), 6 Pa (b), 9 Pa (c), 15 Pa (d), 40 Pa (e) and 50 Pa (f). Data of LYO A and LYO B at different shelf temperatures (0°C and -40°C) were combined.

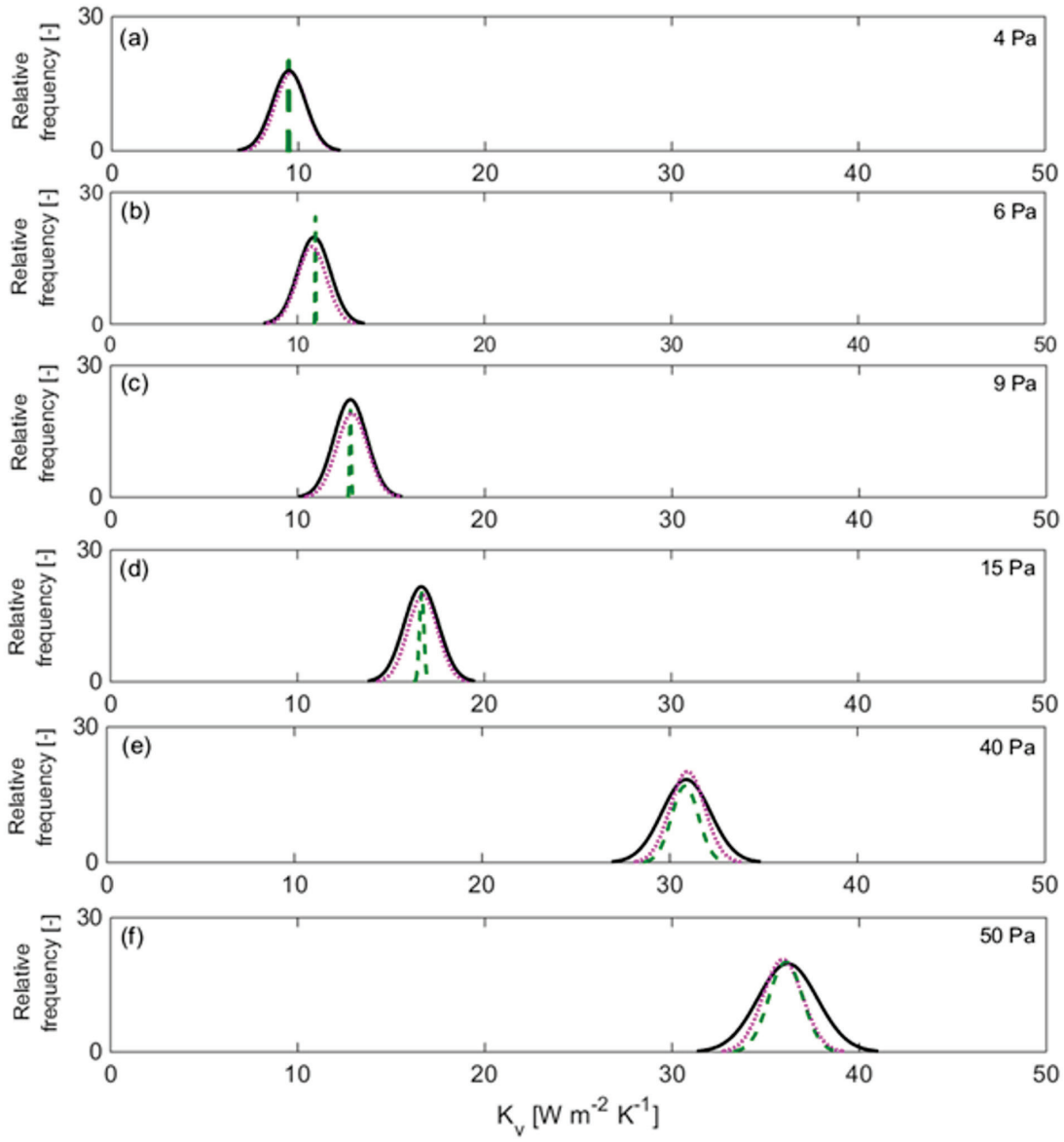


**Figure 6.** Calculated $K_v$ normal distributions: curvature-based (dashed green line – –), contact area-based (dotted red line - - -) and combined curvature and contact area-based (solid black line —) at 4 Pa (a), 6 Pa (b), (c) 9 Pa (c), 15 Pa (d), 40 Pa (e) and 50 Pa (f).

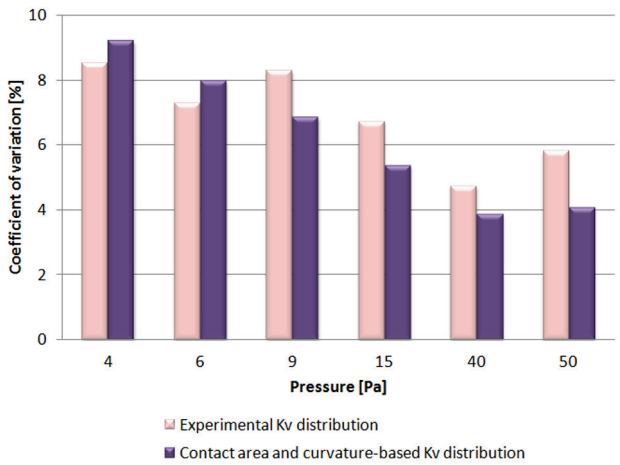


**Figure 7.** Coefficients of variation of experimentally-measured $K_v$ distribution (LYO A and B; light bars) and calculated (combined contact area and curvature-based) $K_v$ distribution (dark bars) and at different pressures.

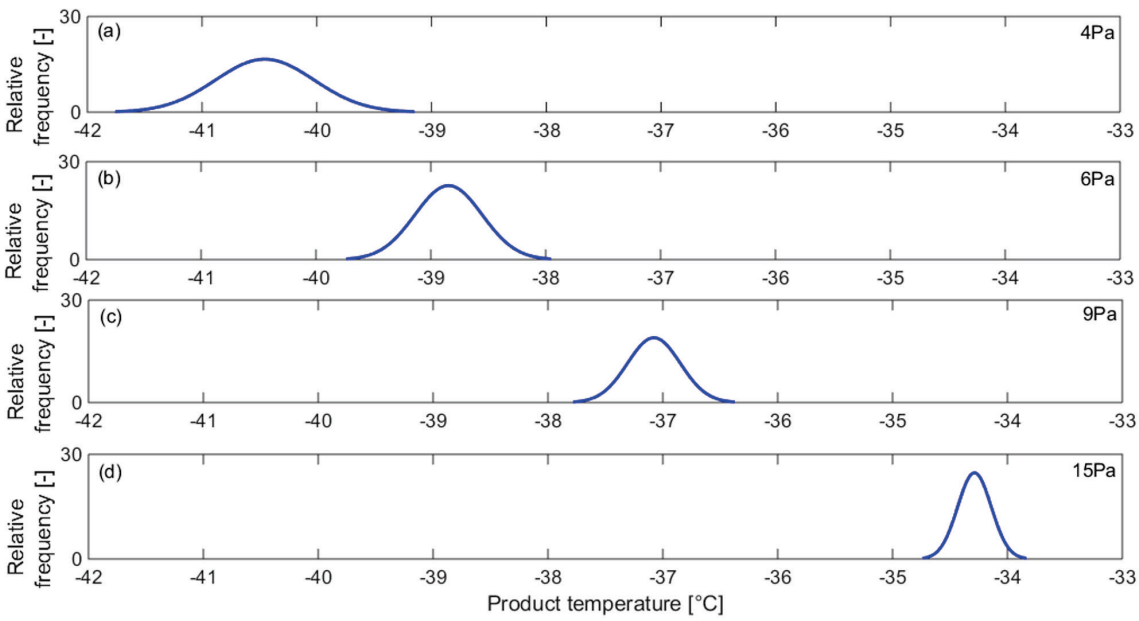


**Figure 8.** Product temperature distributions obtained from the contact area and curvature-based distribution for a 5 % w/w sucrose solution processed at a shelf temperature of -25 °C and four chamber pressures: (a) 4 Pa, (b) 6 Pa, (c) 9 Pa and (d) 15 Pa.

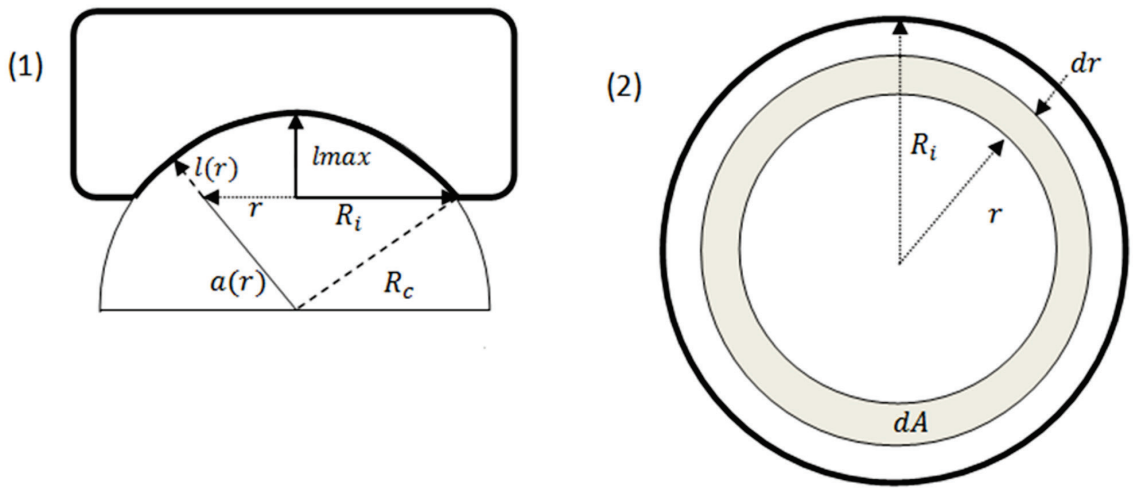


**Figure A.** Side (1) and top (2) view of the vial bottom represented as a semi-spherical calotte.